Appendix

Table A1. Crystal data parameters of Form-I and Form-II. (Chapter 2)

Compound	**Form-I**	**Form-II**
Empirical formula	$C_{15}H_{24}N_8O_5S_3$	$C_{15}H_{24}N_8O_5S_3$
Formula weight	492.60	492.60
Crystal system	orthorhombic	orthorhombic
T [K]	100	100
a [Å]	7.6988(15)	7.8919(8)
b [Å]	14.210(3)	14.0563(14)
c [Å]	20.212(4)	19.110(2)
α [°]	90	90
β [°]	90	90
γ [°]	90	90
Volume [Å^3]	2211.3(8)	2119.8(4)
Space group	$P2_12_12_1$	$P2_12_12_1$
Z	4	4
D_{calc} [gcm^{-3}]	1.480	1.543
μ (mm^{-1})	0.380	0.397
Unique reflections	4245	4156
Observed reflections	2267	3817
R_1 [$I > \sigma(I)$]	0.0645	0.0387
wR_2, GOF	0.1580, 0.866	0.0884, 0.974
Instrument	Bruker APEX-II	Bruker APEX-II
X-ray source	Mo Kα; λ = 0.71073	Mo Kα; λ = 0.71073
CCDC no.	2202507	2208412

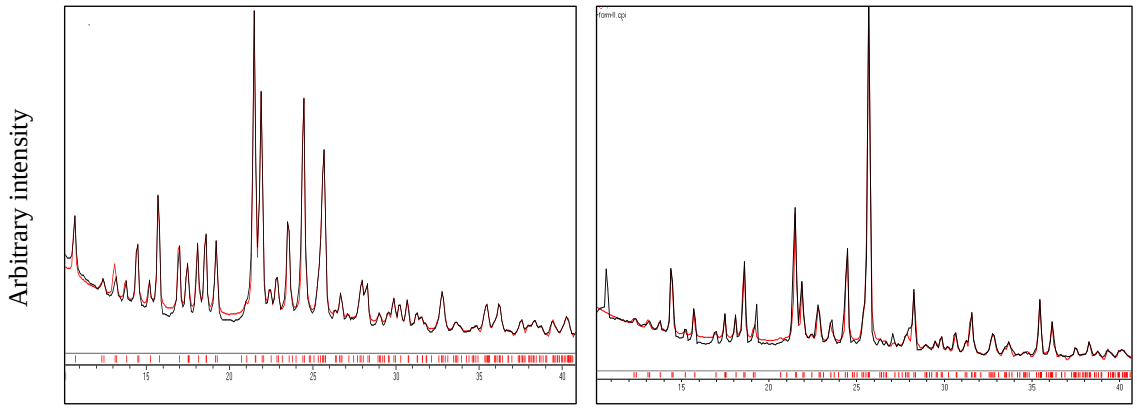

(a) Form-I (b) Form-II

Figure A1. The Rietveld refinement of (a) Form-I and (b) Form-II shows that the experimental (black) and the simulated PXRD (red) agree well, indicating the formation of pure phase for dimorphic forms, Form-I and II.

Table A2. Single crystal X-ray diffraction data of C-1 to C-6. (Chapter 3)

Compound	**C-1**	**C-2**	**C-3**
emp. form.	$C_{15}H_{23}N_7O_6S_3$	$C_{15}H_{23}N_7O_6S_3$	$C_{15}H_{23}N_7O_6S_3$
form. wt.	493.58	493.58	493.58
cryst. syst.	orthorhombic	triclinic	monoclinic
T [K]	100	100	100
a [Å]	8.014(2)	7.8007(6)	8.665(3)
b [Å]	14.172(4)	12.1636(9)	19.932(6)
c [Å]	19.184(6)	12.7573(10)	13.116(4)
α [°]	90	70.408(5)	90
β [°]	90	80.014(5)	105.103(3)
γ [°]	90	75.605(5)	90
V [Å^3]	2178.7(11)	1099.20(15)	2187.2(11)
sp. group	$P2_12_12_1$	$P\bar{1}$	$P2_1$/c
Z	4	2	4
D_{calc} [gcm^{-3}]	1.505	1.491	1.499
μ (mm^{-1})	0.388	0.385	0.387
uni. refls.	5663	4306	4302
obs. refls.	4139	2551	3337
R_1 [$I > \sigma(I)$]	0.0381	0.0548	0.0394
wR_2, GOF	0.0884, 0.949	0.1462, 1.015	0.1037, 1.073
instrument	Bruker APEX-II	Bruker APEX-II	Bruker APEX-II
X-ray	MoKα; λ = 0.71073	MoKα; λ = 0.71073	MoKα; λ = 0.71073
CCDC no.	2202504	2202505	2202506
Refcode	RERCIE	RERCOK	RERCUQ
Compound	**C-4**	**C-5**	**C-6**
emp. form.	$C_{15}H_{24}N_8O_5S_3$	$C_{15}H_{22}N_8O_4S_3$	$C_{15}H_{24}N_8O_5S_3$
form. wt.	492.60	474.58	492.60
cryst. syst.	orthorhombic	monoclinic	monoclinic
T [K]	100	100	100
a [Å]	7.6988(15)	31.478(4)	8.621(5)
b [Å]	14.210(3)	8.5197(11)	20.075(11)
c [Å]	20.212(4)	17.019(2)	13.127(7)
α [°]	90	90	90
β [°]	90	92.841(3)	103.220(7)
γ [°]	90	90	90
V [Å^3]	2211.3(8)	4558.6(10)	2212(2)
sp. group	$P2_12_12_1$	C2/c	$P2_1$/c
Z	4	8	4
D_{calc} [gcm^{-3}]	1.480	1.383	1.479
μ (mm^{-1})	0.380	0.363	0.380

uni. refls.	4245	4428	4350
obs. refls.	2267	4093	2854
R_1 [$I > \sigma(I)$]	0.0645	0.0421	0.0545
wR_2, GOF	0.1580, 0.866	0.0930, 1.056	0.1479, 1.028
instrument	Bruker APEX-II	Bruker APEX-II	Bruker APEX-II
X-ray	MoKα; λ = 0.71073	MoKα; λ = 0.71073	MoKα; λ = 0.71073
CCDC no.	2202507	2202508	2202509
Refcode	RERCEA	RERDAX	RERDEB

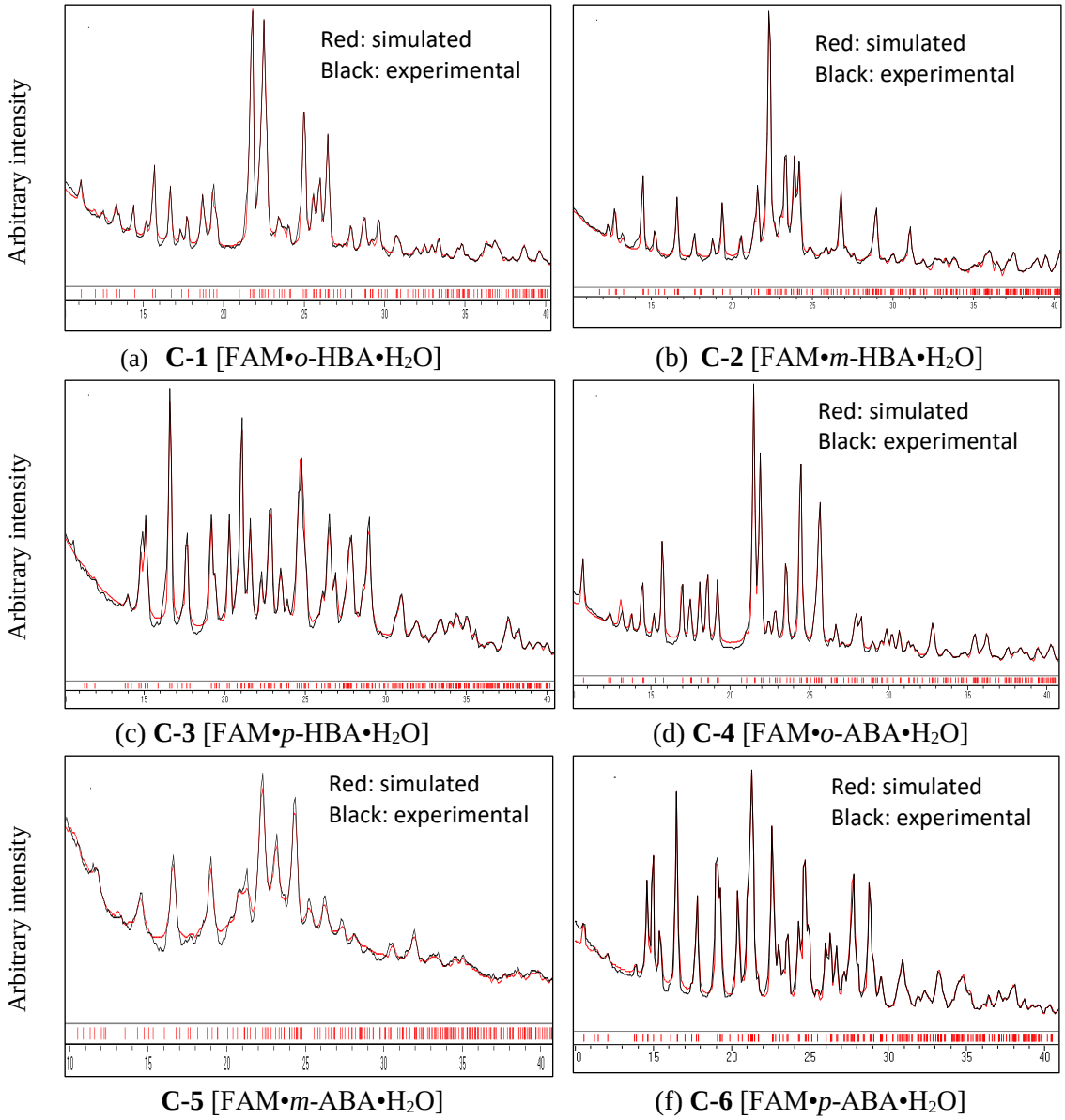

Figure A2. Rietveld refinement of PXRD pattern of C-1 to C-6 (black) with simulated pattern extracted from the corresponding crystal structure (red). For all products, peaks from the experimental bulk materials are matching well with the simulated line from the X-ray crystal structure, indicating bulk materials purity and crystalline phase homogeneity.

Table A3. Change in the torsion angles of FAM in crystal structures of C-1 to C-6

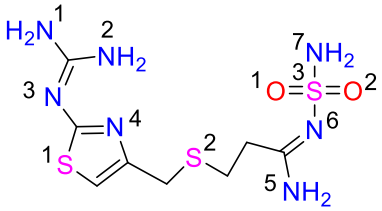

Molecular Conformer	Torsion angle (°)							
	FAM A	FAM B	C-1	C-2	C-3	C-4	C-5	C-6
N4–C4–C5–S2	79.7	63.0	75.3	77.8	55.8	77.1	75.1	62.9
C8–N6–S3–N7	59.36	67.9	82.3	94.7	162.8	80.1	73.5	162.3
C3–C4–C5–S2	101.7	130.7	109.4	98.2	126.7	107.1	102.9	118.5
C5–S2–C6–C7	89.16	172.6	62.1	74.2	63.6	63.2	79.19	59.7
C7–C8–N6–S3	171.98	172.8	173.1	173.2	175.1	173.2	167.61	175.7
C6–C7–C8–N5	100.4	131.5	96.9	81.5	71.9	95.6	172.4	69.1
S2–C6–C7–C8	68.3	72.7	176.7	79.9	38.1	175.8	171.63	41.3

Table A4. Comparison of hydrogen bond synthons observed in FAM molecular salts with the Crystal Structure Database (CSD version 2022.1). Isomeric monoaminobezoic acids and isomeric monohydroxybenzoic acids were used as coformers.

guanidine - COOH	synthon type(s)	guanidine -COOH- SO_2NH_2	synthon type(s)	guanidine -COOH- OH	synthon type(s)	guanidine -COOH $-NH_2$	synthon type(s)
DEBMOM	I	HOLHIC	I	ETIGAP		DUFDOX10	I, II
DUFDOX	I, II	-		JOGVAD	I	HOLHIC	I
DUMPUW	I, II			KIJVEH		NUQREY	I, II
ECANII	I			LABZAP		NUQROI	I, II
ECUTIF				LUDKAW	I	PEDRIB	I
ETIGAP				PEDRIB	I	NUQRUO	I, II
EWAHUH	II			REHTII	II	NUQSAV	II
EZOGAD				SEWXEY		PUNPUK	I
EZOGEH				TUTFIY	I	XUHYUW	I, II
GIPHES	I			VAFXAE	I		
GUHOXM01	I			VOTMEW	I		
HIBDEB				XUHYUW	I, II		
HOLHIC	I			ZEBRAB	I		
JOGVAD	I						
KIJVEH							
LABZAP							
LUDKAW	I						
NUQREY	I, II						
NUQROI	I, II						
PEDRIB	I						
NUQRUO	I, II						
NUQSAV	II						
PUNPUK	I						
QIFFIU	I						
QIFFAO	I						
QISGOR	I						
REHTII	II						
SEWXAU, SEWXEY	I						
TUTFIY	I						
UFALET							

UJOCUS	
VAFXAE	I
VOTMEW	I
XUHYUW*	I, II
ZEBQII	I
ZEBQUU	I
ZEBRAB	I
ZOGCOP*	I

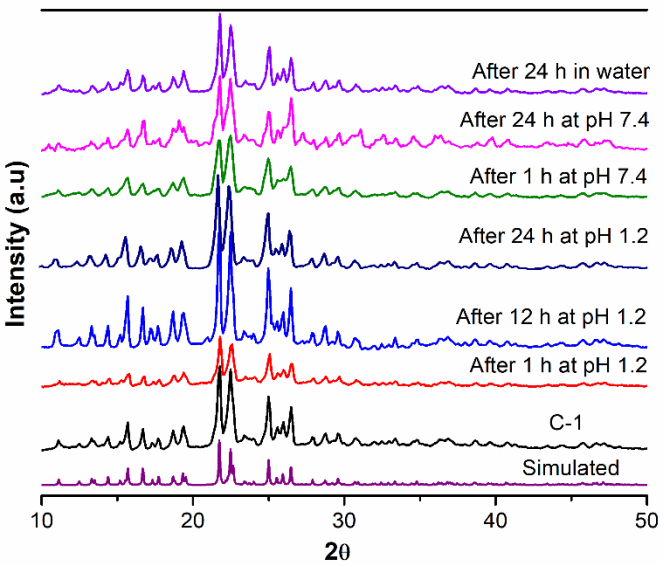

(a) Stacked PXRD patterns of C-1

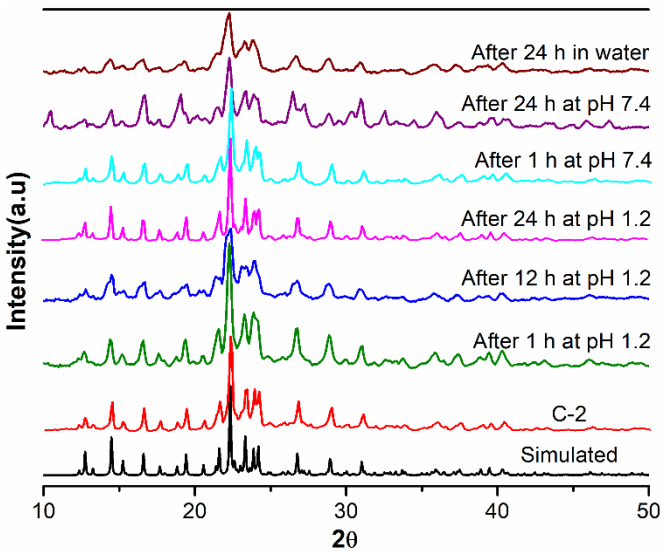

(b) Stacked PXRD patterns of C-2

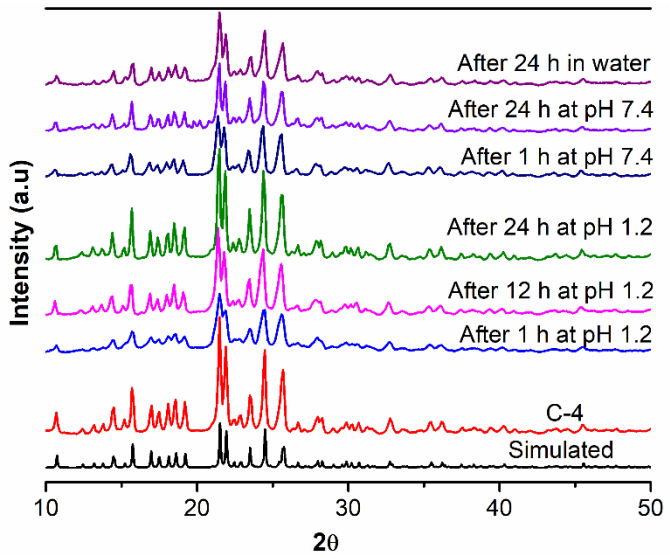

(c) Stacked PXRD patterns of C-4

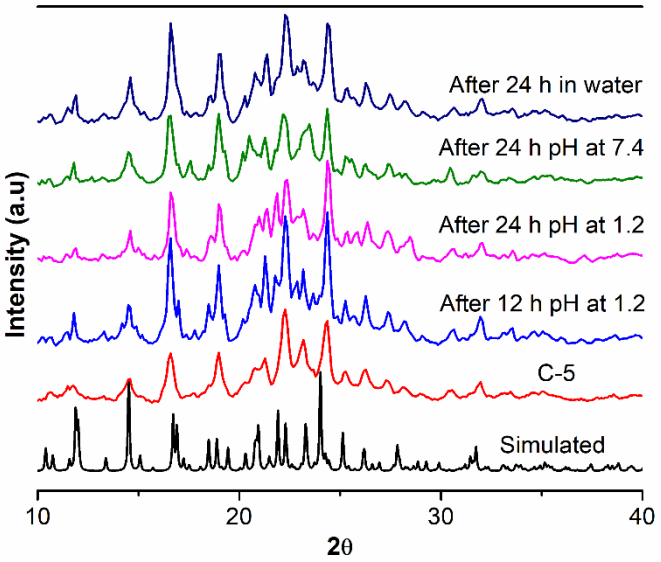

(d) Stacked PXRD patterns of C-5

Figure A3. Phase stability study of C-1, C-2, C-4, and C-5 by a slurry experiment in an aqueous medium and buffer solution of pH 1.2 and 7.4. The constancy of PXRD patterns for all the salts confirms their stability up to 24 h in all three media.

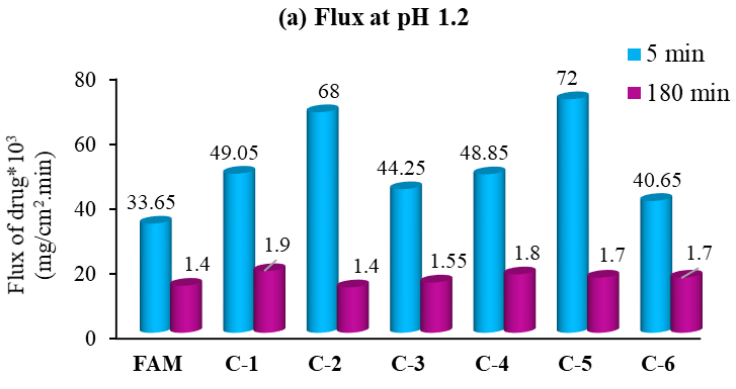

(a)

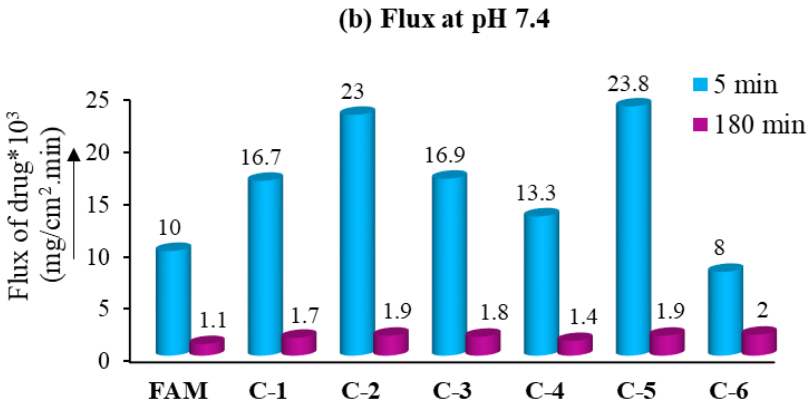

(b)

Figure A4. The amount of drug flux for FAM and its products at (5 min) and 180 min at pH of (a) 1.2 and (b) 7.4

Table A5. Crystallographic parameters for molecular Salts F-23 to F-35. (Chapter 4)

Compound	**F-23**	**F-24**	**F-25**
Emp. form.	$C_{15}H_{25}N_7O_8S_3$	$C_{15}H_{23}N_7O_7S_3$	$C_{16}H_{25}N_7O_7S_3$
Form. Wt.	527.60	509.58	523.61
Cryst. Syst.	Triclinic	Monoclinic	Monoclinic
T [K]	100	100	100
a [Å]	7.19(2)	8.524(4)	5.1507(15)
b [Å]	7.76(2)	20.292(9)	13.468(4)
c [Å]	21.34(6)	13.417(6)	17.168(5)
α [°]	86.11(4)	90	90
β [°]	86.58(4)	103.252(6)	92.848(8)
γ [°]	81.59(3)	90	90
V [Å^3]	1174(6)	2258.9(18)	1189.5(6)
Sp. group	$P\bar{1}$	$P2_1/c$	*P*n
Z	2	4	2
D_{calc}[gcm^{-3}]	1.493	1.498	1.462
μ (mm^{-1})	0.372	0.380	0.363
Uni. Refls.	2623	4444	4682
Obs. Refls	1693	3098	3665
R_1 [$I > \sigma(I)$]	0.0624	0.0587	0.0448
wR_2, GOF	0.1751, 0.995	0.1541, 1.043	0.0981, 1.067
Instrument	Bruker APEX-II	Bruker APEX-II	Bruker APEX-II
X-ray	MoKα; λ = 0.71073	MoKα; λ = 0.71073	MoKα; λ = 0.71073
CCDC no.	2239938	2239941	2239940
Compound	**F-26**	**F-34**	**F-35**
Emp. form.	$C_{15}H_{21}N_7O_6S_3$	$C_{15}H_{25}N_7O_8S_3$	$C_{15}H_{25.5}N_7O_{8.25}S_3$
Form. Wt.	491.57	527.60	532.10
Cryst. Syst.	Monoclinic	Monoclinic	Monoclinic
T [K]	100	100	100
a [Å]	18.723(6)	28.750(3)	17.033(7)

b [Å]	12.794(6)	8.3743(7)	8.125(3)
c [Å]	9.210(4)	21.853(2)	16.574(7)
α [°]	90	90	90
β [°]	105.44(3)	118.402(4)	93.255(10)
γ [°]	90	90	90
V [Å^3]	2126.6(16)	4628.1(8)	2290.0(16)
Sp. group	Cc	C2/c	$P2_1/c$
Z	4	8	4
D_{calc}[gcm^{-3}]	1.535	1.514	1.543
μ (mm^{-1})	0.398	0.377	0.382
Uni. Refls.	4119	4508	4385
Obs. Refls	1928	3859	3847
R_1 [$I > \sigma(I)$]	0.0794	0.0292	0.0823
wR_2, GOF	0.2252, 0.876	0.0712, 0.991	0.1989, 1.090
Instrument	Bruker APEX-II	Bruker APEX-II	Bruker APEX-II
X-ray	MoKα; λ = 0.71073	MoKα; λ = 0.71073	MoKα; λ = 0.71073
CCDC no.	2239939	2239943	2239942

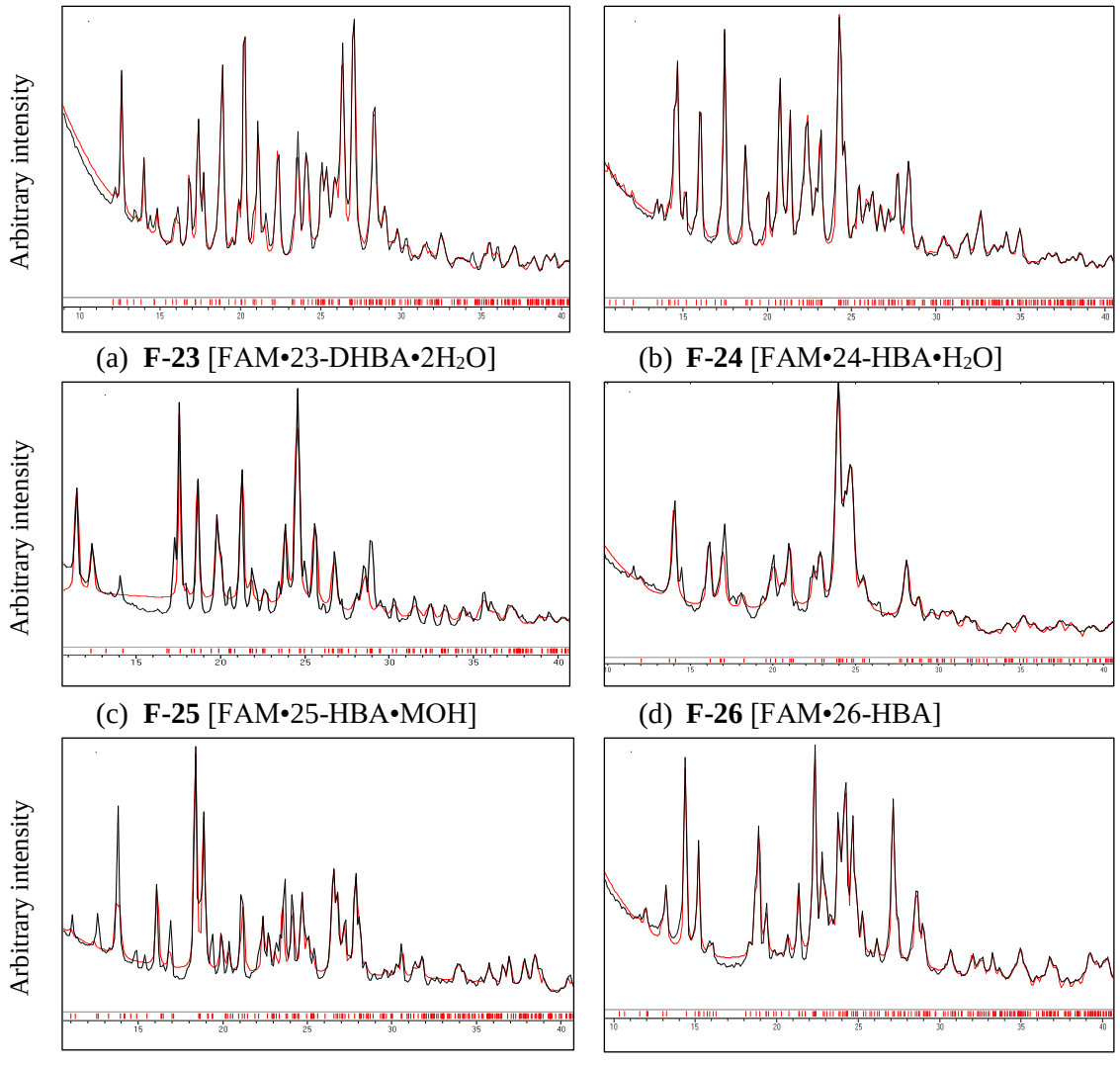

(a) **F-23** [FAM•23-DHBA•2H$_2$O] (b) **F-24** [FAM•24-HBA•H$_2$O]

(c) **F-25** [FAM•25-HBA•MOH] (d) **F-26** [FAM•26-HBA]

(e) **F-34** [FAM•34-HBA•2H$_2$O] (f) **F-35** [FAM•35-HBA•2H2O]

Figure A5. Rietveld refinement of experimental PXRD pattern of F-23 to F-35 (black) with their simulated PXRD profile lines (red).

Table A6. Bond length and bond angle parameters of imine group of guanidine moiety of the FAM and carboxylic acid group in the DHBA of the salt products.

solid form	bond length (Å) & bond angles (°) parameters of imine group			bond length (Å) and bond angle (°) parameters of the COOH group		
	C1–N3	N3–C2	C1–N3–C2	O3–C9	C9–O4	O3–C9–O4
FAM-A	1.33	1.36	120.12	1.24	1.31	122.68
F-23	1.36	1.40	126.14	1.28	1.28	122.02
F-24	1.35	1.38	125.58	1.26	1.27	122.24
F-25	1.35	1.38	12511	1.25	1.27	123.05
F-26	1.37	1.39	126.10	1.26	1.27	124.60
F-34	1.35	1.38	125.08	1.26	1.27	123.01
F-35	1.35	1.38	125.08	1.26	1.27	123.01

Table A7. Comparison of change in the torsion angles of FAM conformers in crystal structures of F-23 to F-35

torsion angle	**angle parameter in different (º)**							
	FAM-A	FAM-B	F-23	F-24	F-25	F-26	F-34	F-35
C8-N6-S3-N7	59.36	67.9	80.7	163.5	86.7	82.2	86.35	71.8
C3-C4-C5-S2	101.7	130.7	77	118.7	134	92.5	119.83	107.1
N4-C4-C5-S2	79.7	63	106	62.5	42.7	87	59.13	74.8
C7-C6-S2-C5	89.16	172.6	150.9	66	85.5	68	67.78	73
C6-C7-C8-N6	77	43	57	103.1	49.7	35	111.9	46.8
C6-C7-C8-N5	100.4	131.5	126.7	74	129.9	144.5	67.8	133.7
S2-C6-C7-C8	68.3	72.7	178.8	36.5	72.5	166	60.86	61.6

Table A8. Crystallographic parameters of the TRM-23 to TRM-35. (Chapter 5)

Compound	**TRM-23**	**TRM-24**	**TRM-25**
Form. unit	$C_{21}H_{20}N_4O_7$	$C_{21}H_{28}N_4O_9$	$C_{21}H_{24}N_4O_7$
Form. wt.	444.40	480.47	444.40
Crys. Sys.	Monoclinic	Monoclinic	Monoclinic
T [K]	100	100	100
a [Å]	6.746(5)	12.0359(4)	7.010(7)
b [Å]	28.380(2)	10.3966(4)	28.22(3)
c [Å]	11.232(9)	19.2847(8)	10.936(11)
α [°]	90	90	90
β [°]	102.929(10)	101.865(2)	103.231(15)
γ [°]	90	90	90
V [Å^3]	2096(3)	2361.58(16)	2106(4)
Space group	$P2_1/n$	$P2_1/c$	$P2_1/n$
Z	4	4	4
D_{calc} [gcm^{-3}]	1.411	1.351	1.402
μ (mm^{-1})	0.109	0.107	0.107
Uni. refls.	3892	4641	3913
Obs. refls.	1750	3132	1596
R_1 [$I > \sigma$(I)]	0.0642	0.0474	0.0702

wR_2	0.1608	0.1349	0.2039
Instrument	Bruker APEX-II	Bruker APEX-II	Bruker APEX-II
X-ray	MoKα; λ = 0.71073	MoKα; λ = 0.71073	MoKα; λ = 0.71073
Compound	**TRM-26**	**TRM-34**	**TRM-35**
Form. unit	$C_{21}H_{24}N_4O_7$	$C_{21}H_{30}N_4O_{10}$	$C_{21}H_{26}N_4O_8$
Form. wt.	444.44	498.49	462.46
Crys. Sys.	Monoclinic	Triclinic	Triclinic
T [K]	100	100	100
a [Å]	25.666(2)	7.229(10)	8.890 (3)
b [Å]	9.2718(7)	9.749(14)	10.737 (5)
c [Å]	19.6923(16)	17.42(3)	13.890 (5)
α [°]	90	79.481(16)	71.237 (7)
β [°]	111.678(5)	78.967(15)	73.526 (7)
γ [°]	90	80.484(16)	67.995(7)
V [Å^3]	4354.8(6)	1173.878	1143.8 (7)
Space group	$C2/c$	$P\bar{1}$	$P\bar{1}$
Z	8	2	2
D_{calc} [gcm^{-3}]	1.356	1.410	1.343
μ (mm^{-1})	0.103	0.113	0.104
Uni. refls.	4053	4367	3057
Obs. refls.	1870	1588	1939
R_1 [$I > \sigma(I)$]	0.0522	0.0782	0.0507
wR_2	0.1478	0.2258	0.1326
Instrument	Bruker APEX-II	Bruker APEX-II	Bruker APEX-II
X-ray	MoKα; λ = 0.71073	MoKα; λ = 0.71073	MoKα; λ = 0.71073

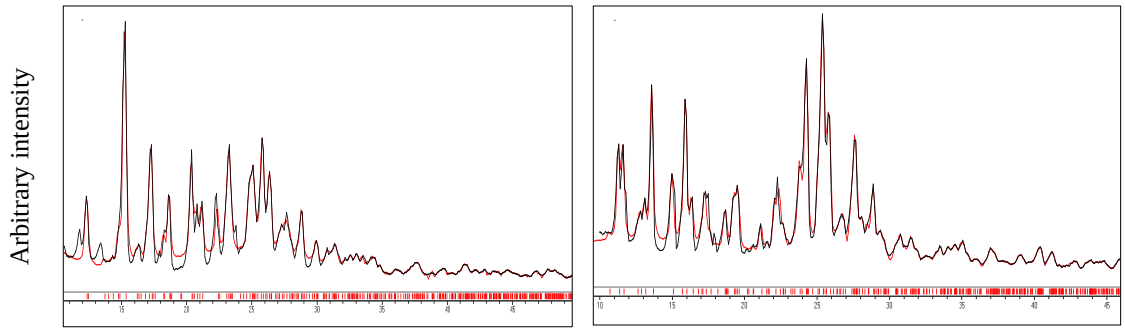

(a) TRM-23 (b) TRM-24

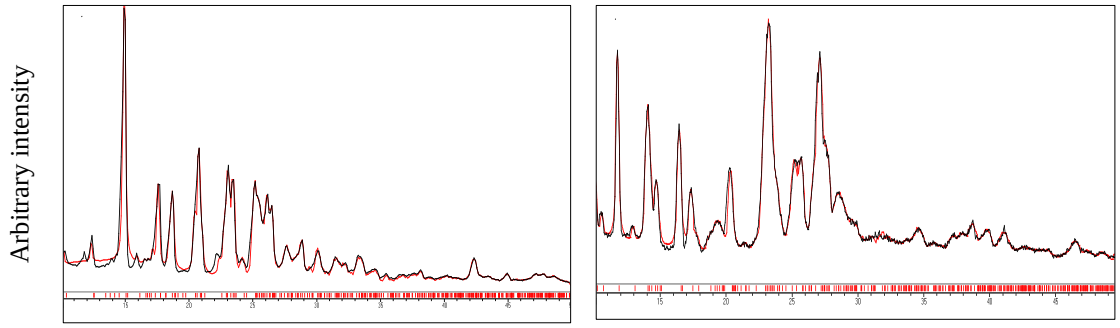

(c) TRM-25 (d) TRM-26

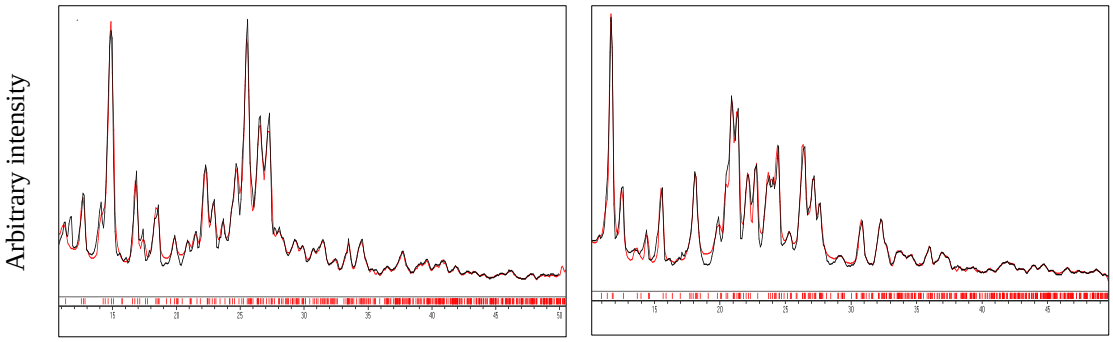

(e) TRM-34 (f) TRM-35

Figure A6. Rietveld refinement of experimental PXRD pattern of TRM-23 to TRM-35 (black) with their simulated PXRD profile lines (red).

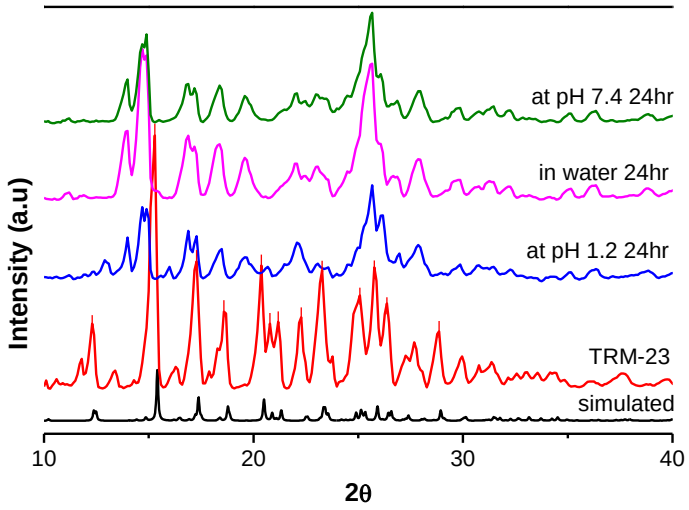

(a) Stability of TRM-23DHBA

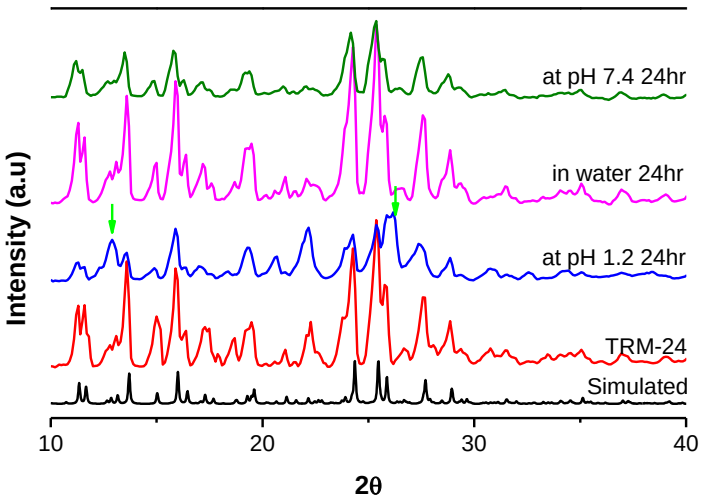

(b) Stability of TRM-24DHBA

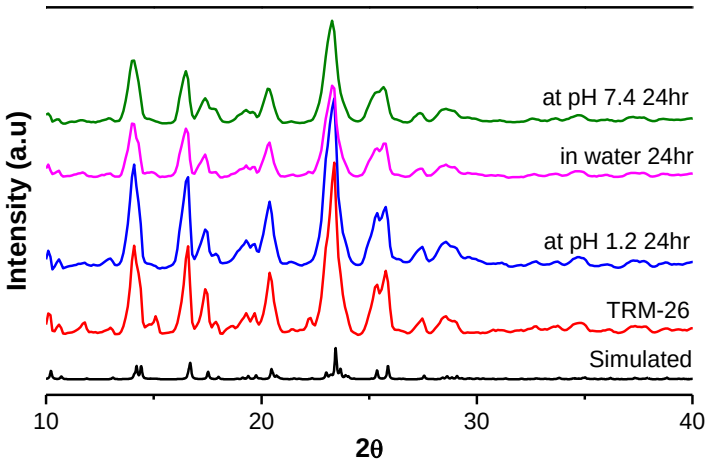

(c) Stability of TRM-26DHBA

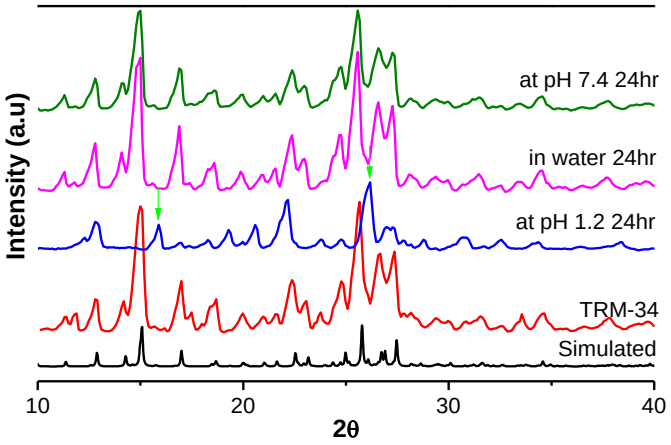

(d) Stability of TRM-34DHBA

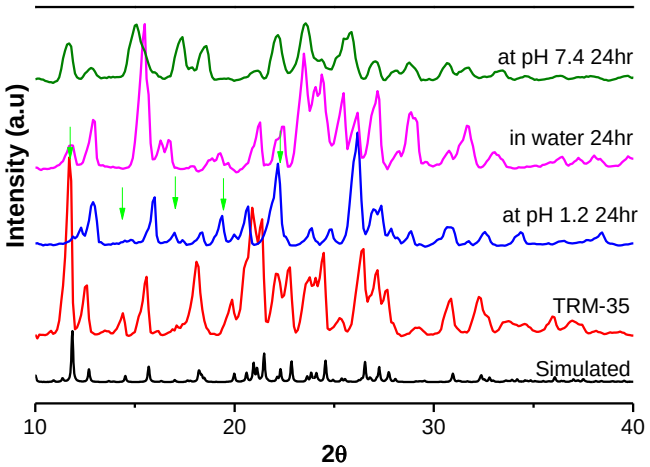

(e) Stability of TRM-35DHBA

Figure A7. The overlaid PXRD patterns of phase stability tests of TRM salts by a slurry experiment in three pH conditions. Except for TRM-24, TRM-34, and TRM-35 at pH 1.2, all the product materials are found to be stable in the three different media at 24 h.

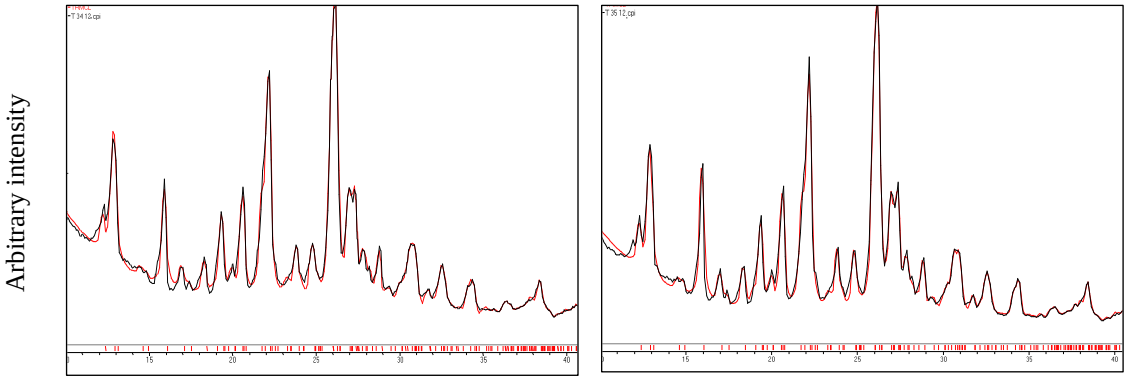

(a) TRM-34 (b) TRM-35

Figure A8. The comparison of PXRD patterns of undissolved materials of TRM-34 and TRM-35 from 1.2 pH medium after 24 h with the simulated PXRD profile of trimethoprim hydrochloride salt.

Table A9. Crystallographic parameters of TRM-1 to TRM-6. (Chapter 6)

Compound	**TRM-1**	**TRM-2**	**TRM-3**	**TRM-4**	**TRM-6**
Form. unit	C_{21} H_{30} N_4 O_9	$C_{21}H_{26}N_4O_7$	$C_{21}H_{28}N_4O_8$	$C_{21}H_{25}N_5O_5$	$C_{21}H_{29}N_5O_7$
Form. wt.	482.49	446.46	464.47	427.46	463.49
Crys. Sys.	Monoclinic	Monoclinic	triclinic	monoclinic	monoclinic
T [K]	100	100	100	100	100
a [Å]	4.9996(15)	6.9248(15)	8.376(7)	6.687(2)	20.253(3)
b [Å]	20.2053(80)	29.213(6)	8.906(8)	28.314(10)	6.0779(6)
c [Å]	23.4768(56)	10.870(2)	17.670(16)	11.091(4)	21.121(3)
α [°]	90	90	85.29(2)	90	90
β [°]	93.87(2)	104.339(6)	82.73(2)	101.754(11)	118.299(18)
γ [°]	90	90	62.79(2)	90	90
V [Å^3]	2366.2(13)	2130.44(35)	1162.5(18)	2055.9(12)	2289.9(6)
Space group	$P2_1/n$	$P2_1/n$	P-1	$P2_1/n$	P $2_1/n$
Z	4	4	2	4	4
D_{calc} [gcm^{-3}]	1.354	1.392	1.327	1.381	1.344
μ (mm^{-1})	0.107	0.106	0.103	0.101	0.102
Uni. refls.	4388	4187	4323	3825	4269
Obs. refls.	1116	2681	3270	2269	1669
R_1 [$I > \sigma(I)$]	0.080	0.071	0.042	0.056	0.069
wR_2	0.27	0.22	0.123	0.168	0.1842
GOF	0.829	1.029	1.080	1.098	0.903
Instrument	Bruker APEX-II	Bruker APEX-II	Bruker APEX-II	Bruker APEX-II	Bruker APEX-II
X-ray	MoKα; λ = 0.71073	MoKα; λ = 0.71073	MoKα; λ = 0.71073	MoKα; λ = 0.71073	MoKα; λ = 0.71073

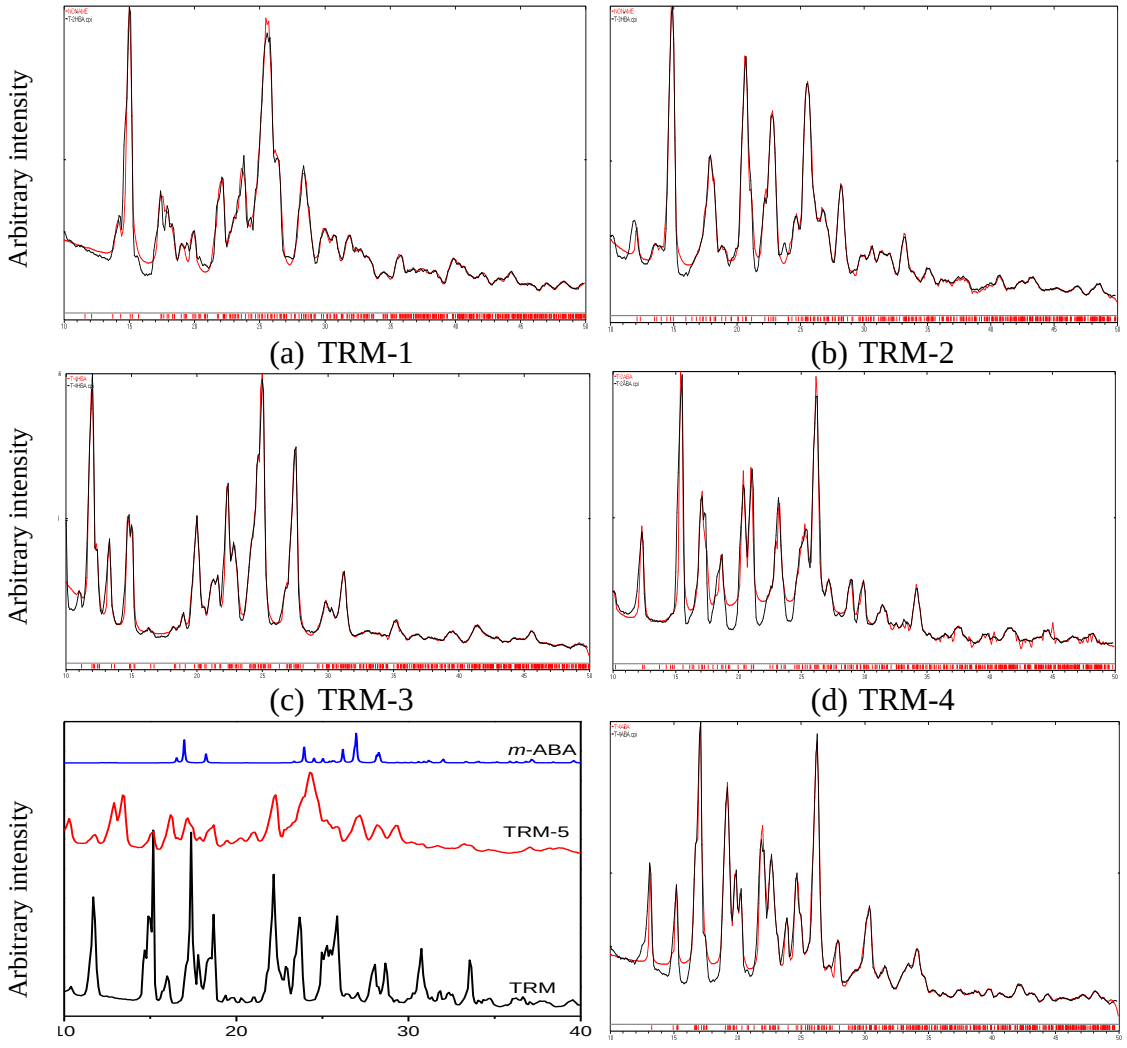

Figure A9. Rietveld refinement of experimental PXRD pattern of TRM-1 to TRM-6 (black) with their simulated PXRD profile lines (red). The PXRD pattern of TRM-5 is compared with its starting materials and found to be different from them.

Figure A10a-c. The phase stability tests of TRM-1 to TRM-6 at pH 1.2 and 7.4 at 12 h.

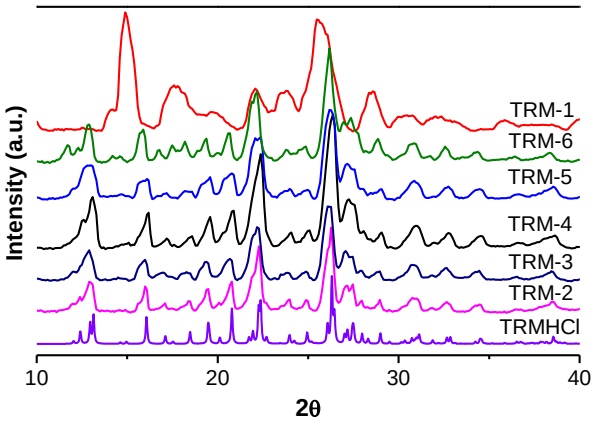

(a) Except for TRM-1, the undissolved materials of salt of TRM from the pH 1.2 at 12 h match with the simulated profile of the reported trimethoprim hydrochloride (Ref. code TMPHCL01).

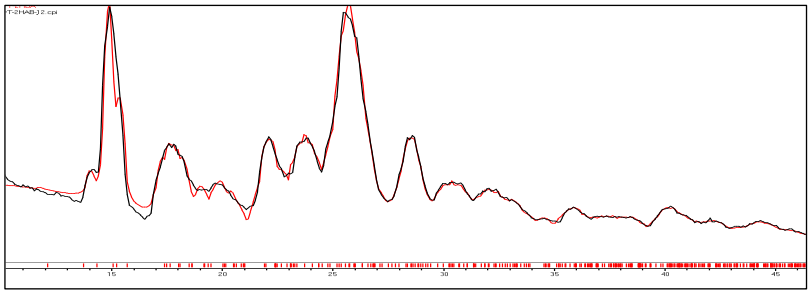

(b) The undissolved material of TRM-1 from the buffer solution of pH 1.2 at 12 h completely matches its simulated PXRD patterns, indicating its stability at this pH condition.

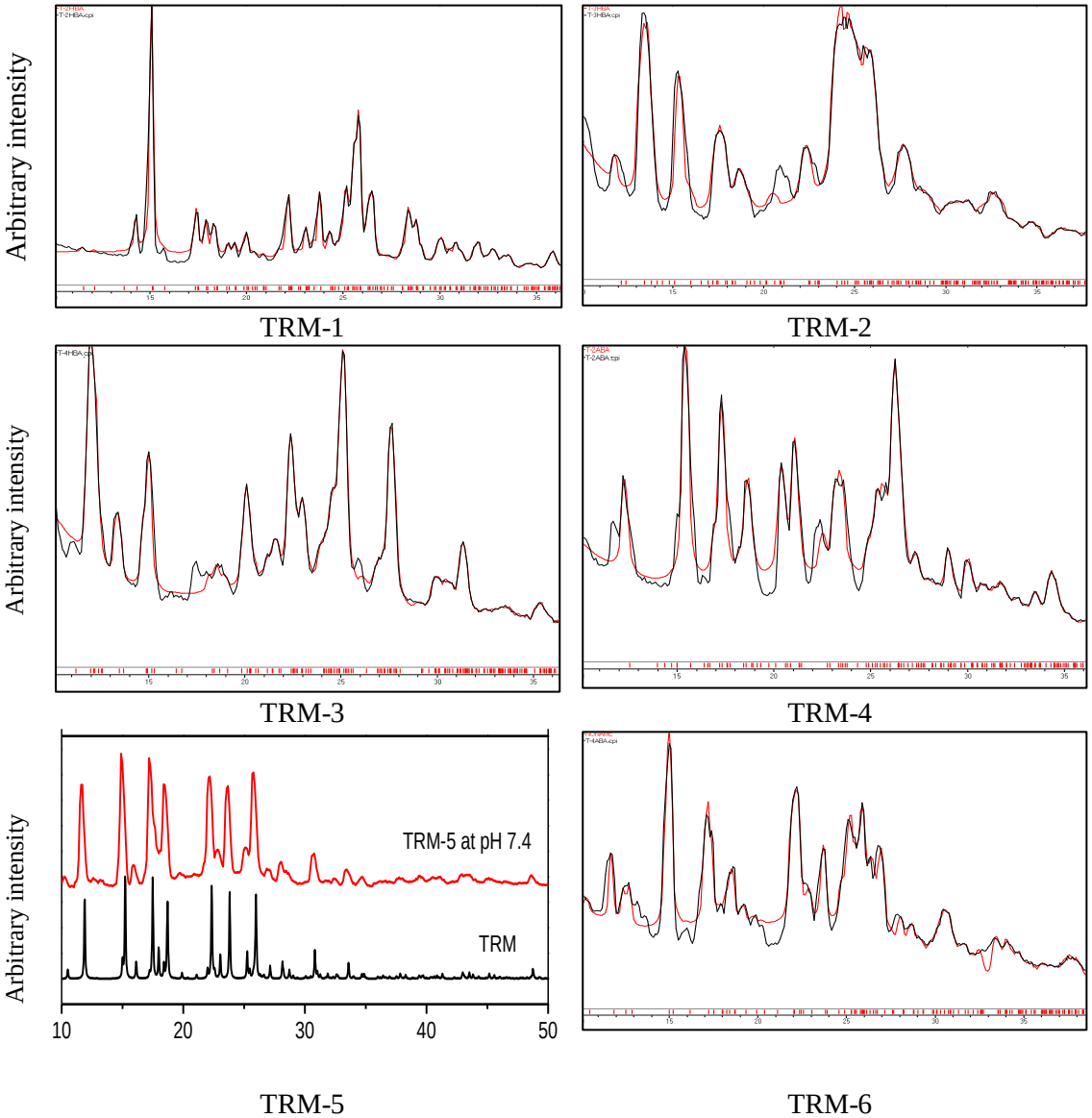

(c) The undissolved products from the buffer solution of pH 7.4 after 12 h matches well with their respective simulated PXRD patterns. But the PXRD profile of the undissolved material of TRM-5 matches with the simulated PXRD patterns of pure TRM (Ref. code AMXBPM10), indicating its dissociation into starting materials.

List of Publications

[1] Zeleke, T. Y. and Sarma, B. Isomeric Coformer Responsive Conformational Adjustment to Recuperate Stability, Solubility, and In Vitro Permeation Behaviour of Drug Molecular Salts. *Crystal Growth & Design,* 22(12):7405–7418, 2022. (https://mjl.clarivate.com:/search-results?issn=1528-7483&hide_exact_match_fl=true&utm_source=mjl&utm_medium=share-by-link&utm_campaign=search-results-share-this-journal)

[2] Zeleke, T. Y. and Sarma, B. Regulating Drug Efficacy by Topological Distribution of N–H···O and O–H···O Interactions in Dimorphic Famotidine Molecular Salts. (Under revision)

[3] Zeleke, T. Y. and Sarma, B. Molecular Salts of Drug Famotidine with Isomeric Dihydroxybenzoic Acids. (Submitted with minor revision)

[4] Zeleke, T. Y. and Sarma, B. Role of Water Molecule(s) of Crystallization in the Modulation of Solubility and Permeation Behaviour of Molecular Salts of Trimethoprim. (Communicated)

[5] Zeleke, T. Y. and Sarma, B. Molecular Salts of Antibiotic Drug Trimethoprim to Improve Its Physicochemical Properties. (Manuscript under preparation)

List of Conferences/Seminars Attended

[1] Zeleke, T. Y. and Sarma, B. *Molecular Salts of Famotidine and Physicochemical Property Studies.* National level seminar on Sustainability, Medicine, and Clean Energy, organized by the Department of Chemical Sciences in association with inSCLgnis'22, Tezpur University, India, March 1, 2022.

[2] Zeleke, T. Y. and Sarma, B. *Improving Stability, Solubility, and In Vitro Permeation Behaviour of drug Famotidine via Molecular Salt formulation*. International conference on frontiers in Chemical Sciences-2022, organized by the Department of Chemistry, IIT Guwahati, India, December 2-4, 2022.

[3] Zeleke, T. Y. and Sarma, B., *Formulation of Stable Molecular Salts of drug Famotidine for the Improvement of its Solubility and Membrane Permeability*. National Seminar on Research at the Interface of Chemical, Biological, and material sciences, organized by the Department of Chemical Sciences, Tezpur University, India, March 10, 2023.